

NUC-MINN-2001/4-T  
February 2001

# Two-Loop Self-Energy and Multiple Scattering at Finite Temperature

J.I. Kapusta<sup>1</sup> and S.M.H. Wong<sup>2</sup>

<sup>1</sup>*School of Physics and Astronomy, University of Minnesota  
Minneapolis, MN 55455*

<sup>2</sup>*Department of Physics, Ohio State University  
Columbus, OH 43210*

## Abstract

One and two loop self-energies are worked out explicitly for a heavy scalar field interacting weakly with a light self-interacting scalar field at finite temperature. The ring/daisy diagrams and a set of necklace diagrams can be summed simultaneously. This simple model serves to illustrate the connection between multi-loop self-energy diagrams and multiple scattering in a medium.

PACS numbers: 11.10.Wx, 11.80.La

The study of how and why the properties of particles change in a thermal medium is fascinating and of particular importance in the areas of cosmology, astrophysics, and high energy nucleus-nucleus collisions. In this paper we investigate a very simple model involving a heavy scalar field with vacuum mass  $M$  interacting with a much lighter scalar field with vacuum mass  $m \ll M$  at temperature  $T \ll M$ . The lighter field has a quartic self-interaction that is stronger than the interaction between the light and heavy fields. Although the model considered here is not realistic it has many properties in common with more physically interesting theories, such as the decay of a very heavy boson in the early universe or the emission of a very massive virtual photon in high energy nuclear collisions. The simplicity of this model allows a very clear mathematical evaluation of the heavy boson self-energy at finite temperature and its physical interpretation in terms of multiple scattering in the many-particle medium. One loop self-energies were studied and physically interpreted in a beautiful paper by Weldon [1]. Some examples of two loop calculations are [2, 3, 4, 5] but since those are oriented toward real physical applications the resulting formulae are necessarily much more involved and oftentimes tedious to reproduce. We should also like to point out that at low to moderate densities the self-energy can always be expressed as an integral over the scattering amplitude for scattering from particles in the medium. Frequently one can use experimental input of scattering amplitudes to construct the self-energy [6]. A formal discussion of this is was presented by Jeon and Ellis [7].

The heavy scalar field is labeled  $H$  and the much lighter scalar field is labeled  $\phi$ . The interaction Lagrangian is

$$\mathcal{L}_I = gH\phi^2 - \lambda\phi^4. \quad (1)$$

The cubic coupling  $g$  has the dimension of mass while the quartic coupling is dimensionless. It is assumed that  $g^2 \ll \lambda M^2$  in order that we can ignore any self-energy diagrams involving an internal  $H$  line. This is analogous to the problem of the coupling of a photon to quarks where the electromagnetic coupling is much smaller than the strong coupling.

The resulting one and two loop diagrams for the  $H$  are drawn in Fig. 1. We are interested in the limit that the  $H$  is at rest with respect to the medium. (The interested reader may easily generalize the results that follow.) We will first evaluate the diagrams in Euclidean space and then analytically continue to Minkowski space. Denoting the Mat-

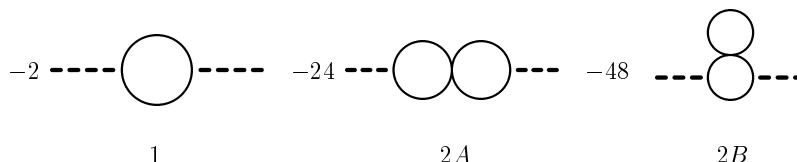


Figure 1: The one and two loop contributions to the  $H$  self-energy under the condition  $g^2 \ll \lambda M^2$ . The thick dashed line is the  $H$ , the solid line is the  $\phi$ . There is a factor  $g$  at each three point vertex and a factor  $-\lambda$  at each four point vertex.

subara frequency of the external  $H$  line by  $\omega_n = 2\pi nT$  we can find explicit mathematical expressions for these diagrams in the usual way [8].

$$\Pi_1 = -2g^2 \left[ T \sum_j \int \frac{d^3p}{(2\pi)^3} \frac{1}{\omega_j^2 + p^2 + m^2} \frac{1}{(\omega_j - \omega_n)^2 + p^2 + m^2} \right] \quad (2)$$

$$\Pi_{2A} = 24g^2\lambda \left[ T \sum_j \int \frac{d^3p}{(2\pi)^3} \frac{1}{\omega_j^2 + p^2 + m^2} \frac{1}{(\omega_j - \omega_n)^2 + p^2 + m^2} \right]^2 \quad (3)$$

$$\begin{aligned} \Pi_{2B} = 48g^2\lambda \left[ T \sum_k \int \frac{d^3q}{(2\pi)^3} \frac{1}{\omega_k^2 + q^2 + m^2} \right] \\ \left[ T \sum_j \int \frac{d^3p}{(2\pi)^3} \frac{1}{\omega_j^2 + p^2 + m^2} \left( \frac{1}{(\omega_j - \omega_n)^2 + p^2 + m^2} \right)^2 \right] \end{aligned} \quad (4)$$

These summations may be evaluated directly or by the use of contour integration.

The simplest summation is

$$F(m, T) = T \sum_j \int \frac{d^3p}{(2\pi)^3} \frac{1}{\omega_j^2 + p^2 + m^2} = \int \frac{d^3p}{(2\pi)^3} \frac{1}{\omega} \left[ n_{\text{BE}}(\omega/T) + \frac{1}{2} \right] \quad (5)$$

where  $\omega = \sqrt{p^2 + m^2}$  and  $n_{\text{BE}}(x) = 1/(e^x - 1)$  is the Bose-Einstein occupation number. The next simplest is

$$\begin{aligned} G(\omega_n, m, T) &= T \sum_j \int \frac{d^3p}{(2\pi)^3} \frac{1}{\omega_j^2 + p^2 + m^2} \frac{1}{(\omega_j - \omega_n)^2 + p^2 + m^2} \\ &= \int \frac{d^3p}{(2\pi)^3} \frac{1}{\omega} \frac{1}{4\omega^2 + \omega_n^2} [2n_{\text{BE}}(\omega/T) + 1] \end{aligned} \quad (6)$$

The final summation needed is

$$T \sum_j \int \frac{d^3p}{(2\pi)^3} \frac{1}{\omega_j^2 + p^2 + m^2} \left( \frac{1}{(\omega_j - \omega_n)^2 + p^2 + m^2} \right)^2 = -\frac{1}{2} \frac{\partial}{\partial m^2} G(\omega_n, m, T). \quad (7)$$

We can express the one and two loop self-energies in terms of these functions.

$$\Pi_1 = -2g^2 G(\omega_n, m, T) \quad (8)$$

$$\Pi_{2A} = 24\lambda g^2 G^2(\omega_n, m, T) \quad (9)$$

$$\Pi_{2B} = -24\lambda g^2 F(m, T) \frac{\partial}{\partial m^2} G(\omega_n, m, T) \quad (10)$$

In Euclidean space the self-energy is real. Note that both the one and two loop contributions can be expressed in terms of one dimensional integrals.

In order to obtain physical quantities, such as the dispersion relation, scattering, decay, and production rates, we must analytically continue to Minkowski space. The retarded self-energy is obtained by the replacement  $\omega_n \rightarrow -iM + \epsilon$  with  $M > 0$  and  $\epsilon \rightarrow 0^+$ . Then

$$Im G = \frac{1}{16\pi} \sqrt{1 - \frac{4m^2}{M^2}} \left[ (n_{BE}(M/2T) + 1)^2 - n_{BE}^2(M/2T) \right] \quad (11)$$

$$Re G = \frac{1}{2\pi^2} P.V. \int_0^\infty \frac{dp p^2}{\omega} \frac{1}{4\omega^2 - M^2} [2n_{BE}(M/2T) + 1] . \quad (12)$$

Here *P.V.* stands for principle value. The 1 following the Bose-Einstein occupancy number in the real part above represents the vacuum contribution. To really evaluate it we should go back to a four dimensional integration over momentum in Euclidean space and place an upper cutoff on the integration, or else analytically continue to  $4 + \epsilon$  dimensions; in either case renormalization would proceed as usual. See the appendix. The term  $(n_{BE} + 1)^2$  in the imaginary part represents the decay  $H \rightarrow \phi\phi$  with the Bose-Einstein enhancement factor in the final state; the term  $n_{BE}^2$  represents the production  $\phi\phi \rightarrow H$ .

The real part of  $\Pi$  represents a shift in the mass squared of the  $H$  and the imaginary part represents the rate of its decay, scattering, or production. It is instructive to consider the limit  $m \ll T \ll M$ .

$$Re G \approx -\frac{T^2}{6M^2} \quad (13)$$

$$F \approx \frac{T^2}{12} + \text{vacuum} \quad (14)$$

The imaginary part of the  $H$  self-energy at the one and two loop order now takes a very simple form.

$$Im \Pi = -\frac{g^2}{8\pi} \left[ (n_{BE} + 1)^2 - n_{BE}^2 \right] \left\{ 1 + (4 - 2)\lambda \frac{T^2}{M^2} + \dots \right\} \quad (15)$$

This formula may be interpreted thusly. The overall sign results from the convention used for the self-energy. A minus sign indicates loss or decay of the  $H$ , a plus sign indicates gain or production. The factor  $(n_{BE} + 1)^2$  shows the Bose-Einstein enhancement of the final state, the factor  $n_{BE}^2$  shows that the probability of production is proportional to the probability to find two  $\phi$  of the requisite energy in the initial state. (The  $n_{BE}$  are of course evaluated at the energy  $M/2$ .) The correction to order  $\lambda$  has contributions from the diagrams  $\Pi_{2A}$  giving the factor 4 and from  $\Pi_{2B}$  giving the factor  $-2$ . Is there a simple interpretation of these results?

The imaginary part can be obtained by cutting a diagram in half. Cutting the one loop diagram, as in Fig. 2, illustrates the physical process of decay of the  $H$  into  $\phi\phi$ . (For definiteness we focus on the absorption or decay processes. Reversing the in and out states gives the production rate.)

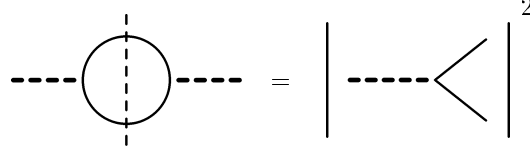


Figure 2: Cutting the one loop self-energy diagram.

Cutting the diagram for  $\Pi_{2A}$  does not yield the square of an amplitude. Instead it illustrates an interference between an amplitude of order zero and an amplitude of order  $\lambda$ . See Fig. 3. Note that there should be a spectator  $\phi$  with energy  $\omega$  in the simpler half of the interference graphs as shown in previous work [9, 10]. We have not included it here to reduce the number of sub-figures within each figure that need to be drawn. The same also applies to Fig. 4 below. The loop that is not cut involves a Matsubara sum. This can be expressed as a vacuum loop plus a finite temperature piece. The former is just the order  $\lambda$  correction to the vertex coupling the  $H$  to  $\phi\phi$ . The latter can be viewed as the absorption of a  $\phi$  from the heat bath with energy  $\omega$  and momentum  $\mathbf{p}$  and the emission of a  $\phi$  into the heat bath with the same energy and momentum. The initial and final states are the same as in the amplitude of lower order in  $\lambda$  provided a spectator is included in the simpler half of the interference graph as mentioned above, hence the reason that it can interfere. There are two diagrams with a single intermediate off-shell  $\phi$ . The kinematics are such that one of them has propagator  $1/q_+^2$  with  $q_+^2 = M(M + 2\omega)$ , and the other has propagator  $1/q_-^2$  with  $q_-^2 = M(M - 2\omega)$ . Adding these two propagators gives  $2/(M^2 - 4\omega^2)$ . This is precisely the origin of the mathematical expressions displayed in eqs. (6) and (12) above.

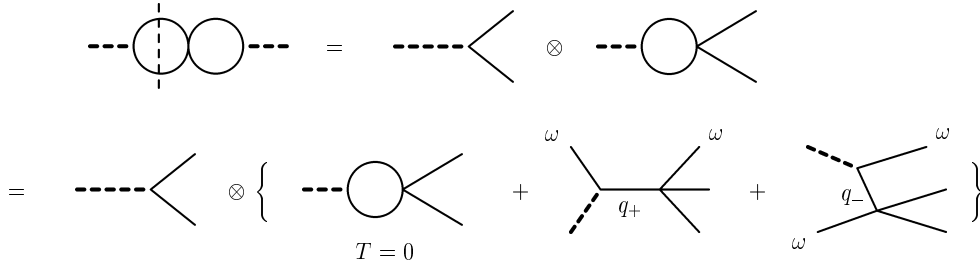


Figure 3: Cutting the two loop diagram for  $\Pi_{2A}$  results in an interference between two amplitudes of different order in  $\lambda$ . A loop involves a Matsubara sum unless otherwise indicated as a vacuum loop. The  $q_+$  and  $q_-$  are the four-momenta of intermediate states. Combinatoric factors are not displayed.

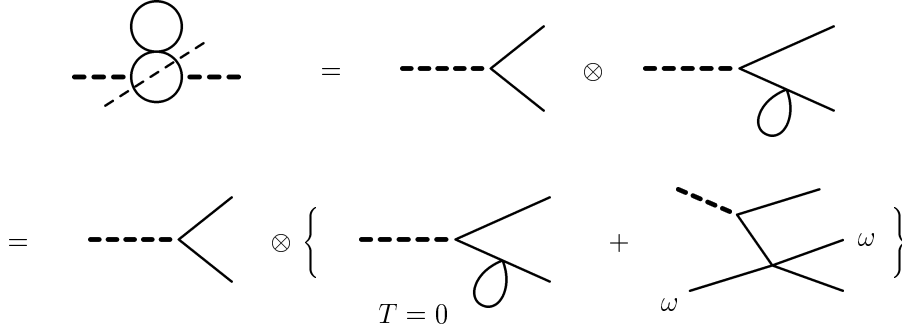


Figure 4: Cutting the two loop diagram for  $\Pi_{2B}$  is just the second term in the Taylor series expansion for the one loop diagram shown in figure 2 with the bare  $\phi$  propagator replaced by the dressed one. In effect the in and out  $\phi$  lines should be dressed to represent collective excitations in the thermal medium rather than vacuum particles.

Cutting the diagram for  $\Pi_{2B}$  is shown in Fig. 4. Again there is an interference between amplitudes of different order in  $\lambda$ . One is tempted to interpret this as scattering of a particle from the heat bath with one of the outgoing  $\phi$  from the  $H$  decay. However, because there is an intermediate line on-shell the diagram is not well-defined mathematically (one should also read the paragraph near the end of the paper which discusses how in the imaginary-time formalism the contour integral allows one to avoid this problem altogether). This should be no surprise: one does not dress external lines when evaluating Feynman diagrams for scattering or decay. Indeed, this diagram really arises from an expansion of  $\Pi$  in terms of a dressed  $\phi$  propagator and bare vertices rather than an expansion in terms of a bare  $\phi$  propagator and bare vertices. The one loop contribution to the self-energy of the  $\phi$  is momentum and frequency independent and is simply given by  $12\lambda F(m, T)$ . The dressed propagator is  $1/(\omega_j^2 + p^2 + m_T^2)$  where  $m_T^2 = m^2 + 12\lambda F(m, T)$ . One sees very clearly that  $\Pi_{2B}$  is the second term in a Taylor series, the first term being  $\Pi_1$ . All diagrams of this type can easily be summed by making the replacement  $\Pi_1(\omega_n, m, T) \rightarrow \Pi_1(\omega_n, m_T, T)$ . Physically what is happening is that the  $H$  is decaying into collective excitations with the quantum numbers of the  $\phi$  rather than into vacuum-like  $\phi$  excitations. In the context of gauge theories this goes by the name of *hard thermal loops* [11]. It is left as an exercise for the reader to show that the combinatoric factor for each diagram in this class is exactly reproduced by this selective resummation. Such perturbative diagrams go by the name of ring or daisy diagrams. One can go even further by summing super ring or super daisy diagrams by solving the integral equation

$$\overline{m}_T^2 = m^2 + 12\lambda F(\overline{m}_T, T) \quad (16)$$

for the effective mass  $\overline{m}_T$ . Examples of ring/daisy and super ring/daisy diagrams are shown in Fig. 5 (a) and (b) respectively.

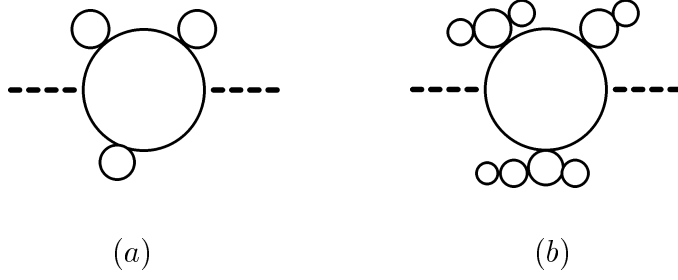


Figure 5: (a) an example of a ring/daisy diagram, and (b) an example of a super ring/daisy diagram.

There is another class of diagrams that are easily summable. We refer to these as necklace diagrams. They have exactly the same topological form as  $\Pi_{2A}$  but with  $N$  loops instead of 2. The overall combinatoric factor is  $-12^N/6$ . The expression for the one with  $N$  loops is

$$\Pi_N^{\text{necklace}} = -\frac{12^N}{6} g^2 (-\lambda)^{N-1} G^N(\omega_n, m, T). \quad (17)$$

This is a geometric series readily summed to give

$$\Pi_{\text{necklace}} = -\frac{2g^2 G(\omega_n, m, T)}{1 + 12\lambda G(\omega_n, m, T)}. \quad (18)$$

Cutting the  $N = 3$  necklace, for example, leads to the diagrams shown in Fig. 6 and Fig. 7. At first one thinks that summing the necklaces amounts to a temperature coupling for  $H\phi\phi$ , namely,  $g^2(T)$ . This is not a good way to think because not only would this effective coupling have a dependence on the external Matsubara frequency  $\omega_n$  but it will become complex when analytically continuing to Minkowski space.

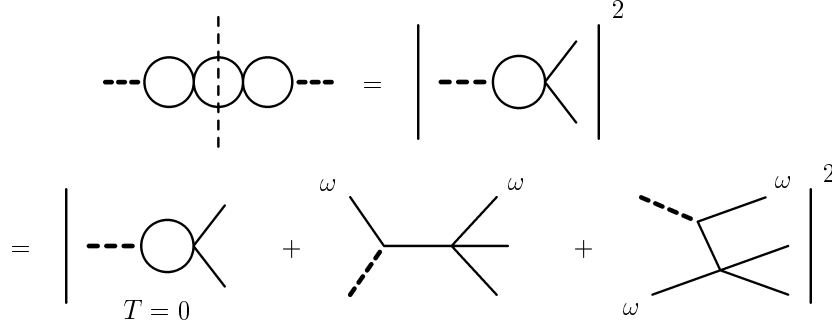


Figure 6: One way of cutting the  $N = 3$  necklace diagram. Combinatoric factors are not displayed.

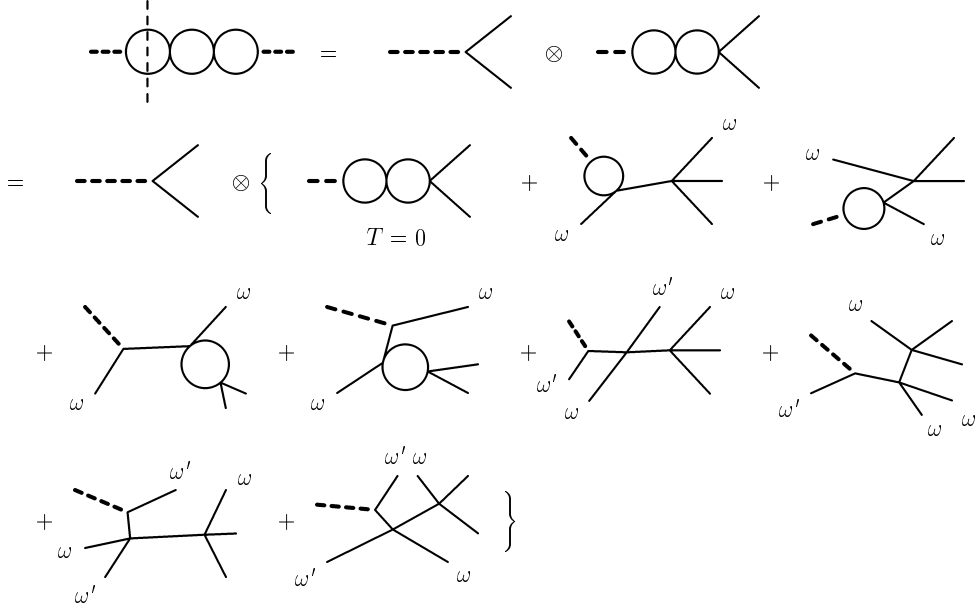


Figure 7: Another way of cutting the  $N = 3$  necklace diagram. All the loops between the brackets are evaluated at  $T=0$ . Combinatoric factors are not displayed.

One can further sum all diagrams of the ring and necklace types simultaneously simply by replacing  $m$  in the necklace formula with  $\overline{m}_T$ .

$$\Pi_{\text{ring+necklace}} = -\frac{2g^2 G(\omega_n, \overline{m}_T, T)}{1 + 12\lambda G(\omega_n, \overline{m}_T, T)}. \quad (19)$$

Neglecting the denominator, and expanding the numerator to zeroth and first order in  $\lambda$  reproduces  $\Pi_1$  and  $\Pi_{2B}$ , respectively. Keeping the numerator to zeroth order and expanding the denominator to first order reproduces  $\Pi_{2A}$ .

We can also calculate the imaginary part for Fig. 1 from the scattering amplitudes shown in Figs. 2-4. This procedure was used in [9] and described in more detail in [10]. Rather than calculating the loop diagrams in Euclidean space, analytically continuing to Minkowski space, and then finding the imaginary part, this procedure uses the scattering amplitudes as input and does a thermal averaging over particles in the heat bath. In this procedure, every line carrying a distinct 4-momentum is integrated over phase space with the appropriate thermal weight. The integrations are of course constrained by a global 4-momentum conserving delta-function. The amplitudes are evaluated at tree level, except for the explicit vacuum loops. There are no finite temperature loops. The amplitudes are computed according to conventional vacuum field theory. In those cases where an outgoing line is in effect dressed by the scattering of a particle from the heat bath, as in Fig. 4, then the amplitude will have to be dealt with more carefully; see below and also ref. [10] for a general discussion.



Applying the scattering amplitude method to the current calculation of the decay of the heavy scalar field  $H$  at rest, one starts directly with the interference graphs on the second line in Fig. 3. A phase space integration measure is assigned to each independent incoming and outgoing line except, of course, the  $H$  line. The two lines carrying the energy  $\omega$  will have only one and *not* two integral measures because the same 4-momentum flows through them. They come from the heat bath and go back into it with the same momentum, therefore they are not constrained by the overall energy-momentum conservation. The contribution from Fig. 3 to the decay rate  $\Gamma$  can be written as

$$2E\Gamma_{\text{(Fig. 3)}} = \frac{1}{2} \int \frac{d^3 p_1}{(2\pi)^3 2p_1^0} \int \frac{d^3 p_2}{(2\pi)^3 2p_2^0} (2\pi)^4 \delta^{(4)}(P - p_1 - p_2) \\ \times \left(1 + n_{\text{BE}}(p_1^0/T)\right) \left(1 + n_{\text{BE}}(p_2^0/T)\right) \left(\mathcal{M}_{\text{tree}}^* \otimes \mathcal{M}_{\text{(Fig. 3)}} + \text{h. c.}\right). \quad (20)$$

The factor of minus one-half is a symmetry factor. Here  $P = (E, \mathbf{P})$  is the 4-momentum of the  $H$ . In this paper, though, we specialize to the  $H$  at rest so that  $\mathbf{P} = 0$  and  $P^0 = M$ . For the simpler half of the interference graph,  $\mathcal{M}$  is just the tree amplitude

$$\mathcal{M}_{\text{tree}} = 2g. \quad (21)$$

The other half is more complicated.

$$\mathcal{M}_{\text{(Fig. 3)}} = 2! \times 4! \times g(-\lambda) \int \frac{d^3 k}{(2\pi)^3 2\omega} \left(\frac{1}{2} + n_{\text{BE}}(\omega/T)\right) \left(-\frac{1}{q_+^2} - \frac{1}{q_-^2}\right) \\ = \frac{4g\lambda T^2}{M^2} + \{T = 0 \text{ part}\} + \mathcal{O}(1/M^4). \quad (22)$$

The factors  $2!$  and  $4!$  come from the  $H\phi^2$  vertex and the  $\phi^4$  vertex, respectively. The  $(1/2 + n_{\text{BE}})$  is the distribution assigned to boson lines which correspond to absorption and emission of the same 4-momenta within the same Feynman graph according to one of the rules given in [10]. Its origin is really just the same as Eq. (5). The denominators  $q_+^2$  and  $q_-^2$  introduced earlier come out automatically from calculating the last two graphs in Fig. 3. They have a minus sign because of our conventions, namely, the propagator is positive in Euclidean space [8]. With Eq. (21) and Eq. (22), Eq. (20) can easily be evaluated to give

$$2M\Gamma_{\text{(Fig. 3)}} = \frac{\lambda g^2 T^2}{\pi M^2} + \{T = 0 \text{ part}\} + \{\text{non-leading terms}\}. \quad (23)$$

The other contribution to the  $H$  decay comes from the processes shown in Fig. 4. This time there is an intermediate line which is on-shell because it carries the same 4-momentum as an outgoing line. For that line, with 4-momentum  $p_1$ , the phase space integral measure must be written out as a 4-momentum integral measure because there is a differentiation of the mass-shell constraining delta-function. The intermediate on-shell

line is mathematically absorbed into this differentiation of the mass-shell constraint and does not appear anywhere else in the calculation. In terms of the self-energy loop diagrams shown in Fig. 1, this derivative of a Dirac delta-function has its origins in a double pole arising from a self-energy insertion. The contribution from Fig. 4 can be written as

$$2M\Gamma_{(\text{Fig. 4})} = \frac{1}{2} \times 2 \int \frac{d^4 p_1}{(2\pi)^4} \int \frac{d^3 p_2}{(2\pi)^3 2p_2^0} 2\pi \delta'^{(+)}(p_1^2) (2\pi)^4 \delta^{(4)}(P - p_1 - p_2) \\ \times \left(1 + n_{\text{BE}}(p_1^0/T)\right) \left(1 + n_{\text{BE}}(p_2^0/T)\right) \left(\mathcal{M}_{\text{tree}}^* \otimes \mathcal{M}_{(\text{Fig. 4})} + \text{h. c.}\right). \quad (24)$$

The factor of two here is for the emission and absorption to occur on either of the two outgoing lines.  $\mathcal{M}_{\text{tree}}$  is the same as above in Eq. (21). The symbol  $\delta'^{(\pm)}$  means to differentiate the Dirac delta-function with respect to its argument, taking the energy positive. The remaining half of the amplitude which contains the emission and absorption is

$$\mathcal{M}_{(\text{Fig. 4})} = 2! \times 4! \times g(-\lambda) \int \frac{d^3 k}{(2\pi)^3 2\omega} \left(\frac{1}{2} + n_{\text{BE}}(\omega/T)\right) \\ = -2g\lambda T^2 + \{T = 0 \text{ part}\}. \quad (25)$$

The factors of  $2!$  and  $4!$  have the same origin as before, and the emission/absorption is associated with a distribution of  $(1/2 + n_{\text{BE}})$ . The integration in Eq. (24) has to be evaluated with some care in order to manipulate correctly the differentiation of the mass-shell constraint. The result is

$$2M\Gamma_{(\text{Fig. 4})} = -\frac{\lambda g^2 T^2}{2\pi M^2} + \{T = 0 \text{ part}\} + \{\text{non-leading terms}\}. \quad (26)$$

So we have

$$2M\left(\Gamma_{(\text{Fig. 3})} + \Gamma_{(\text{Fig. 4})}\right) \simeq (2-1) \frac{\lambda g^2 T^2}{2\pi M^2} + \{T = 0 \text{ part}\}. \quad (27)$$

The result from Eq. (15) can be recovered with

$$\Gamma = \Gamma_{(\text{Fig. 2})} + \Gamma_{(\text{Fig. 3})} + \Gamma_{(\text{Fig. 4})} \quad (28)$$

using the identification

$$2M\Gamma \left(\exp(-M/T) - 1\right) = 2 \text{ Im } \Pi. \quad (29)$$

One point in the calculation that should be elaborated concerns self-energy insertions. In terms of scattering amplitudes it amounts to dressing an external line, thereby causing a singularity on an internal line. The usual Feynman rules for scattering theory say that external lines should not be dressed but should be taken into account in the phase space. (In our example, this is the intermediate line in Fig. 4.) This usually leads to the need to include at least part of the thermal self-energy in the field, and therefore changes the

mass-shell of the particle. This was shown quite elegantly by Weldon [12] for fermions. Donoghue and Holstein have done the same but in a Lorentz non-covariant manner [13]. When calculating loops in the imaginary-time formalism, there is a rigorous solution to this problem. It is well-known that the contour integral method has a well-defined way of dealing with multi-pole singularities. The residue of the multi-pole is found by differentiating the non-pole part of the integrand by one power less than that of the order of the multi-pole. So, if one insists on no resummation of any sort, including those of super ring/daisy diagrams mentioned above, or even partial resummation, such as those of Weldon, Donoghue and Holstein, then the contour method is a good solution to the above problem. This method was also used in [9, 10].

In conclusion we have accomplished several goals. First, we have explicitly evaluated the two loop self-energy for a massive boson weakly interacting with lighter bosons in thermal equilibrium among themselves. This was done first in the imaginary time formalism of Matsubara. There is no ambiguity in analytically continuing to real time or real energies, as first proven by Baym and Mermin 40 years ago [14]. Second, a physical interpretation was found for all diagrams considered. Some of these involve Bose-Einstein enhancement of strongly interacting particles in the final state of the heavy boson decay. Some of them involve absorption and emission of particles from the heat bath with the same energy and momentum. Such processes may interfere with processes of other order in the stronger coupling  $\lambda$ . Third, it was seen how important it is to expand in terms of resummed or interacting propagators. This indicates the importance of identifying the collective excitations of the system. These are all features that must be understood and taken into account when considering the kinetic theory of quark-gluon plasma in heavy ion collisions or in the early universe, for example. Then the role of quarks and gluons are analogous to the  $\phi$  bosons, and the role of the  $H$  is analogous to the electromagnetic field.

## Acknowledgements

This work was supported by the US Department of Energy under grant DE-FG02-87ER40328. S.W. would like to thank the Physics Department at Ohio State University for support.

## References

- [1] H.A. Weldon, Phys. Rev. D 28, 2007 (1983).
- [2] J. Kapusta, P. Lichard, and D. Seibert, Phys. Rev. D **44**, 2774 (1991).
- [3] E. Braaten, R.D. Pisarski, and T.-C. Yuan, Phys. Rev. Lett. **64** 2242 (1990).

- [4] R. Baier, H. Nakkagawa, A. Niegawa, and K. Redlich, Phys. Rev. D **45**, 4323 (1992).
- [5] S.M.H. Wong, Z. Phys. C **53**, 465 (1992); *ibid.*, **58**, 159 (1993).
- [6] E. V. Shuryak, Nucl. Phys. **A533**, 761 (1991); V. L. Eletsky and B. L. Ioffe, Phys. Rev. Lett. **78**, 1010 (1997); V. L. Eletsky and J. I. Kapusta, Phys. Rev. C **59**, 2757 (1999).
- [7] S. Jeon and P.J. Ellis, Phys. Rev. D **58**, 045013 (1998).
- [8] J.I. Kapusta, *Finite Temperature Field Theory* (Cambridge University Press, Cambridge, England, 1989); Phys. Rev. D **46**, 4749 (1992).
- [9] J.I. Kapusta and S.M.H. Wong, Phys. Rev. D **62**, 037301 (2000); Phys. Rev. C **62**, 027901 (2000).
- [10] S.M.H. Wong, Phys. Rev. D, in press (preprint hep-ph/0007212).
- [11] R.D. Pisarski, Nucl. Phys. **B309**, 476 (1988); Phys. Rev. Lett. **63**, 1129 (1989); E. Braaten and R.D. Pisarski, Nucl. Phys. **B337**, 569 (1990).
- [12] H.A. Weldon, Phys. Rev. D **26**, 2789 (1982).
- [13] J.F. Donoghue and B. R. Holstein, Phys. Rev. D **28**, 340 (1983).
- [14] G. Baym and N. D. Mermin, J. Math. Phys. **2**, 232 (1961).
- [15] P. Ramond, *Field Theory: A Modern Primer* (Frontiers in Physics: Vol. 74, Addison-Wesley Pub. Co., rev. ed. 1990).
- [16] R.D. Field, *Applications of Perturbative QCD* (Frontiers in Physics: Vol. 77, Addison-Wesley Pub. Co., 1989).

# Appendix

In this appendix we compute the vacuum self-energy of the  $H$  boson to one and two loop orders. The diagrams are those shown in Fig. 1. We use dimensional regularization (see, for example, chapter 4 of [15]) and take the mass  $m$  of the  $\phi$  boson to be zero for simplicity of presentation. The two integrals which are needed are the  $F$  and  $G$  as displayed in eqs. (2-10). In Euclidean space:

$$F_{\text{vac}} = (\mu^2)^{2-\omega} \int \frac{d^{2\omega}l}{(2\pi)^{2\omega}} \frac{1}{l^2} \quad (30)$$

and

$$G_{\text{vac}} = (\mu^2)^{2-\omega} \int \frac{d^{2\omega}l}{(2\pi)^{2\omega}} \frac{1}{l^2} \frac{1}{(l-P)^2}. \quad (31)$$

Here  $l$  is the loop momentum and  $P$  is the external momentum, both Euclidean. The number of dimensions is  $2\omega$  with  $2-\omega = \epsilon \rightarrow 0^+$ , and  $\mu$  is the dimensional parameter which is arbitrary. Dimensional regularization gives  $F_{\text{vac}} = 0$ .

Using the Feynman parametrization one arrives at

$$\begin{aligned} G_{\text{vac}} &= \frac{\Gamma(\epsilon)}{(4\pi)^2} \left( \frac{4\pi\mu^2}{P^2} \right)^\epsilon \int_0^1 \frac{dx}{[x(1-x)]^\epsilon} = \frac{1}{(4\pi)^2} \left\{ \frac{1}{\epsilon} + \left[ 2 - \gamma_E + \ln \left( \frac{4\pi\mu^2}{P^2} \right) \right] \right. \\ &+ \left[ 4 - \frac{\pi^2}{12} - 2\gamma_E + \frac{1}{2}\gamma_E^2 + (2 - \gamma_E) \ln \left( \frac{4\pi\mu^2}{P^2} \right) + \frac{1}{2} \ln^2 \left( \frac{4\pi\mu^2}{P^2} \right) \right] \epsilon \\ &+ \mathcal{O}(\epsilon^2) \Big\}. \end{aligned} \quad (32)$$

Analytic continuation to Minkowski space involves the replacements  $P^2 \rightarrow -P^2$  and  $\ln(4\pi\mu^2/P^2) \rightarrow \ln(4\pi\mu^2/P^2) + i\pi$ . This results in  $G_{\text{vac}}$  having both real and imaginary parts.

The imaginary part of the  $H$  vacuum self-energy can easily be found from the above results in conjunction with eqs. (8-10). At one loop order

$$\text{Im } \Pi_1^{\text{vac}} = -\frac{g^2}{8\pi} \quad (33)$$

and at two loop order

$$\text{Im } \Pi_2^{\text{vac}} = \frac{3\lambda g^2}{16\pi^3} \left\{ \frac{1}{\epsilon} + 4 - 2\gamma_E + 2 \ln \left( \frac{4\pi\mu^2}{P^2} \right) \right\}. \quad (34)$$

This needs a counterterm added to the Lagrangian to render it finite in the limit  $\epsilon \rightarrow 0$ . We have the freedom to choose the counterterm such that the order  $\lambda$  correction vanishes on the mass-shell. If we make this choice then

$$\text{Im } \Pi_2^{\text{vac}} = \frac{3\lambda g^2}{8\pi^3} \ln \left( \frac{M^2}{P^2} \right), \quad (35)$$

where  $M$  is the physical mass of the  $H$  boson. In effect this defines the normalization point of the coupling  $g$  of the  $H$  to two  $\phi$  mesons. The sum of one and two loops is

$$Im \Pi_{\text{vac}} = -\frac{g^2(M^2)}{8\pi} \left[ 1 - \frac{3\lambda}{\pi^2} \ln \left( \frac{M^2}{P^2} \right) \right] \approx -\frac{1}{8\pi} \frac{g^2(M^2)}{1 + \frac{3\lambda}{\pi^2} \ln \left( \frac{M^2}{P^2} \right)} = -\frac{g^2(P^2)}{8\pi}. \quad (36)$$

This involves the renormalization group running coupling. It displays infrared freedom,  $g^2(P^2) \rightarrow 0$  as  $P^2 \rightarrow 0$ , and the Landau pole at  $P^2 = M^2 \exp(\pi^2/3\lambda)$ .

The above results can also be obtained from the vacuum diagrams shown in Figs. 2 to 4. The methods for doing this are well known: see, for example, chapter 2 of [16]. This is left as an exercise for the reader.